Figure S1

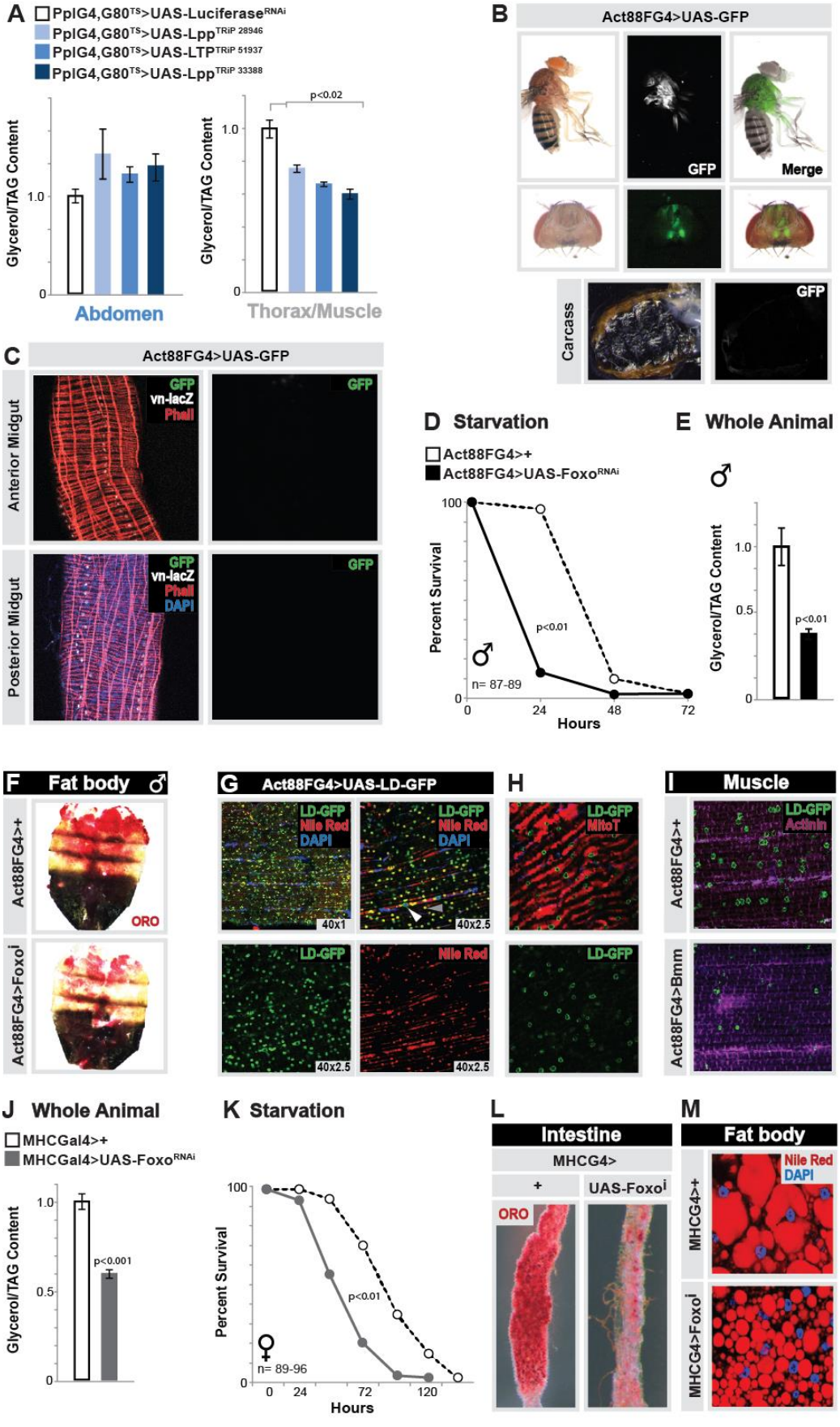
A
PplG4,G80TS>UAS-LuciferaseRNAi
PplG4,G80TS>UAS-LppTRiP 28946
PplG4,G80TS>UAS-LTPTRiP 51937
PplG4,G80TS>UAS-LppTRiP 33388
Glycerol/TAG Content
1.0
0
Abdomen
p<0.02
Thorax/Muscle
B
Act88FG4>UAS-GFP
GFP
Merge
Carcass
C
Act88FG4>UAS-GFP
Anterior Midgut
Posterior Midgut
GFP
vn-lacZ
PhaII
DAPI
D Starvation
Act88FG4>+
Act88FG4>UAS-FoxoRNAi
Percent Survival
100
p<0.01
n= 87-89
0
24
48
72
Hours
E Whole Animal
0.5
p<0.01
F Fat body
Act88FG4>+
Act88FG4>Foxoi
ORO
G Act88FG4>UAS-LD-GFP
LD-GFP
Nile Red
DAPI
40x1
40x2.5
H
MitoT
I Muscle
Actnin
Act88FG4>Bmm
J Whole Animal
MHCGal4>+
MHCGal4>UAS-FoxoRNAi
p<0.001
K Starvation
120
L
Intestine
MHCG4>
+
UAS-Foxoi
M
Fat body
MHCG4>+
MHCG4>Foxoi

Figure S2

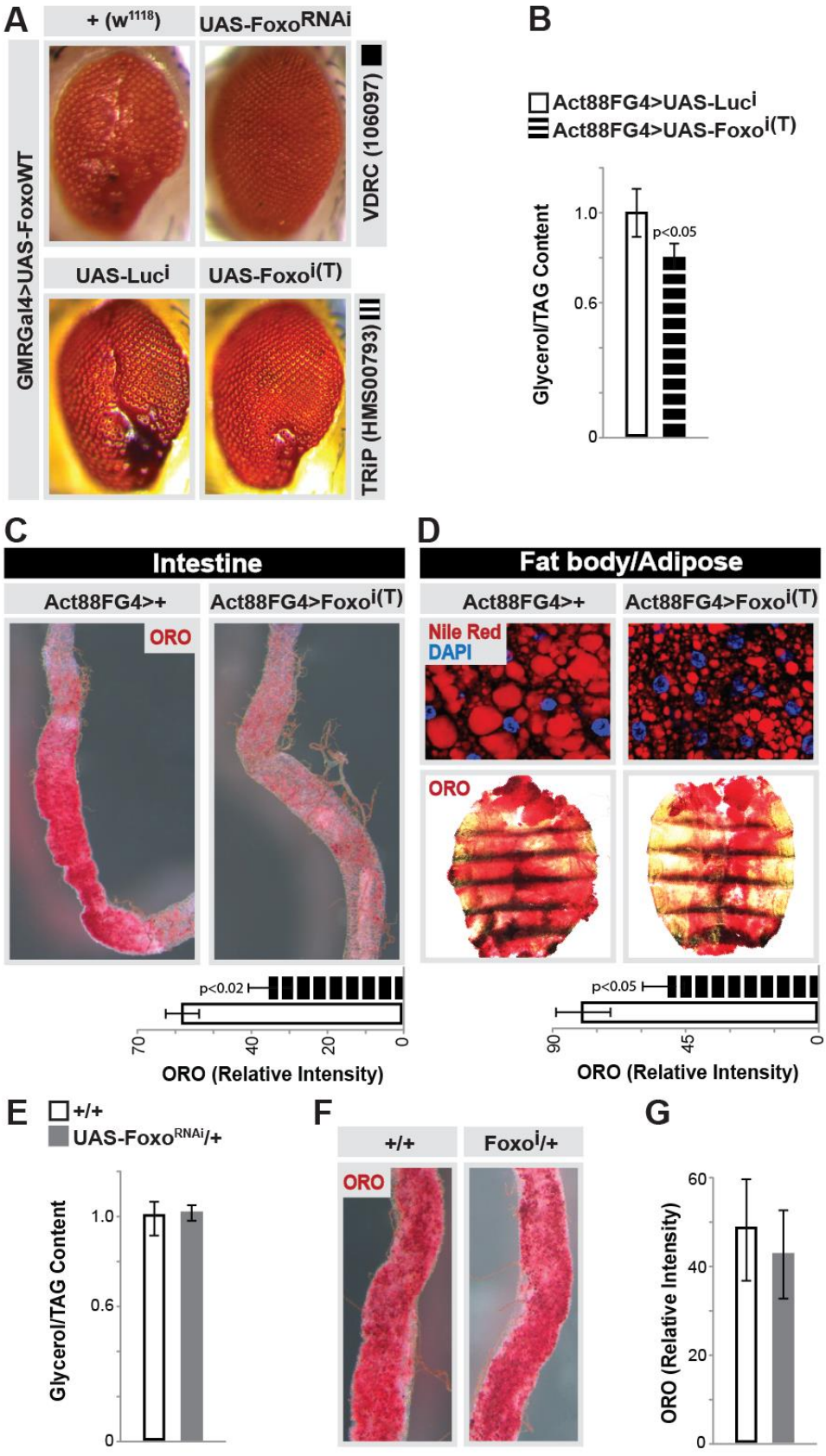
A
+ (w1118)
UAS-FoxoRNAi
GMRGal4>UAS-FoxoWT
VDRC (106097)
UAS-Luci
UAS-Foxoi(T)
TRiP (HMS00793)
B
Act88FG4>UAS-Luci
Act88FG4>UAS-Foxoi(T)
Glycerol/TAG Content
1.0
0.6
0
p<0.05
C
Intestine
Act88FG4>+
Act88FG4>Foxoi(T)
ORO
p<0.02
70
40
20
0
ORO (Relative Intensity)
D
Fat body/Adipose
Act88FG4>+
Act88FG4>Foxoi(T)
Nile Red
DAPI
ORO
p<0.05
90
45
0
ORO (Relative Intensity)
E
+/+
UAS-FoxoRNAi/+
Glycerol/TAG Content
1.0
0.6
0
F
+/+
Foxoi/+
ORO
G
ORO (Relative Intensity)
60
40
20
0

Figure S3

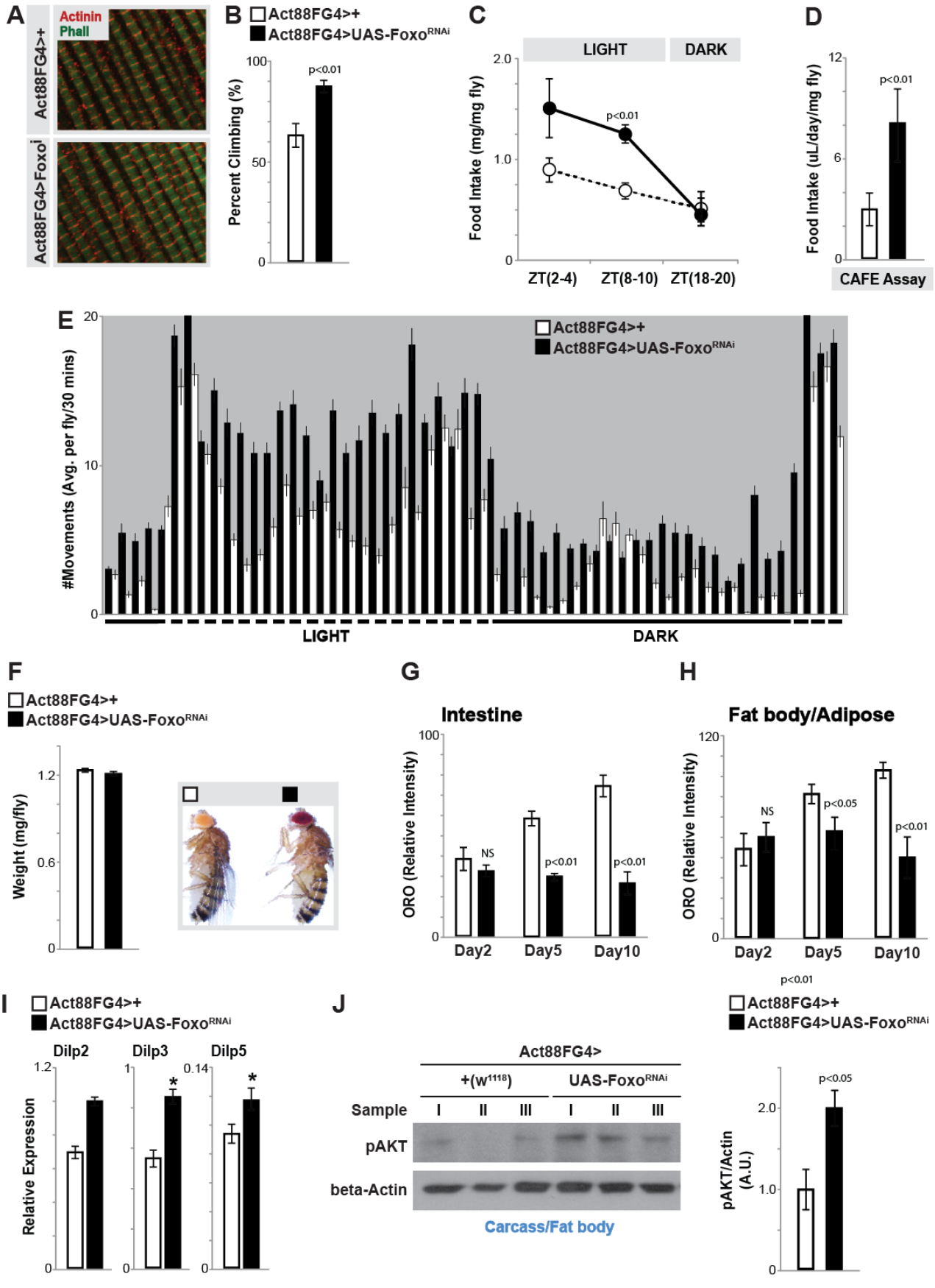
A
Actinin
Phall
Act88FG4>+
Act88FG4>Foxo
B
Act88FG4>+
Act88FG4>UAS-FoxoRNAi
Percent Climbing (%)
p<0.01
C
LIGHT
DARK
Food Intake (mg/mg fly)
p<0.01
ZT(2-4)
ZT(8-10)
ZT(18-20)
D
Food Intake (uL/day/mg fly)
p<0.01
CAFE Assay
E
Act88FG4>+
Act88FG4>UAS-FoxoRNAi
#Movements (Avg. per fly/30 mins)
LIGHT
DARK
F
Act88FG4>+
Act88FG4>UAS-FoxoRNAi
Weight (mg/fly)
G
Intestine
ORO (Relative Intensity)
NS
p<0.01
p<0.01
Day2
Day5
Day10
H
Fat body/Adipose
ORO (Relative Intensity)
NS
p<0.05
p<0.01
Day2
Day5
Day10
I
Act88FG4>+
Act88FG4>UAS-FoxoRNAi
Dilp2
Dilp3
Dilp5
Relative Expression
J
Act88FG4>+
Act88FG4>UAS-FoxoRNAi
Act88FG4>
+(w1118)
UAS-FoxoRNAi
Sample
I
II
III
I
II
III
pAKT
beta-Actin
Carcass/Fat body
p<0.01
pAKT/Actin (A.U.)
p<0.05

Figure S4

A

	RPKM Values					
	Act88FG4>					
	+ (w^{1118})	$Foxo^{RNAi}$	+ (w^{1118})	$Foxo^{RNAi}$	+ (w^{1118})	$Foxo^{RNAi}$
Gene Name	Thorax/Muscle		Intestine		Carcass/Fat body	
RpLP2	1630	1797	2532	2463	3360	4238
RpL21	1394	1467	1503	1631	2830	2644
RpLP1	1480	1603	2065	1682	2407	2892
RpS18	1154	1136	1414	1289	2014	2250
RpS3A	926	796	746	801	1890	1763
RpS30	834	822	1174	1088	1737	1551
RpL15	992	897	1049	971	1710	1520
RpL8	910	1046	1287	1075	1672	2174
RpS2	726	823	1138	989	1668	2397
RpL7	960	990	1021	934	1661	1980
Act5C	166	281	1837	2791	431	537
Gapdh1	514	589	244	223	609	511
Fer1HCH	446	324	1510	2400	501	521
Fer2LCH	423	375	1461	2235	457	533

B

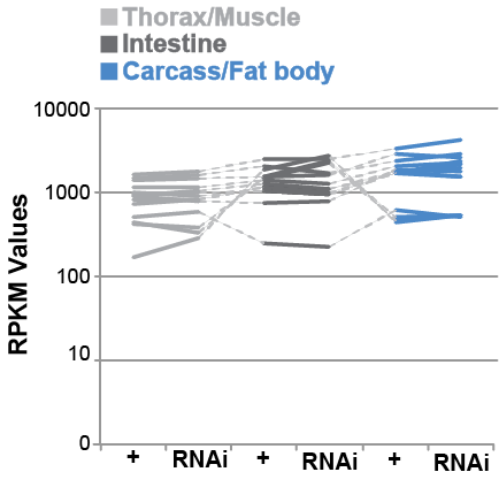

C

	RPKM Values		
	Act88FG4>		
	+ (w^{1118})	+ (w^{1118})	+ (w^{1118})
Gene Name	Thorax/Muscle	Intestine	Carcass/Fat body
lambdaTry	0.695	912.494	7.895
kappaTry	0.177	583.219	3.399
zetaTry	0.291	210.064	0.673
etaTry	0.303	278.554	1.259
thetaTry	0.527	978.901	1.764
epsilonTry	1.928	6404.093	3.914
iotaTry	0.607	205.198	1.246
Act88F	3392.774	1.395	3.345
Mhc	154.197	5.902	35.761
Mlp60A	105.035	12.171	14.122
Mlc1	300.957	12.896	33.041
Act57B	3048.743	69.562	327.471
Mlc2	2282.070	43.285	102.399
Lsd-1	155.302	23.908	587.738
Jabba	52.987	4.166	230.751
FASN1	188.989	26.667	682.252
FASN3	24.749	1.194	249.969
ACC	31.872	9.581	111.805
Fad2	110.730	12.418	1283.225
EloF	43.842	5.968	685.164
CG16904	46.522	6.898	607.852

D

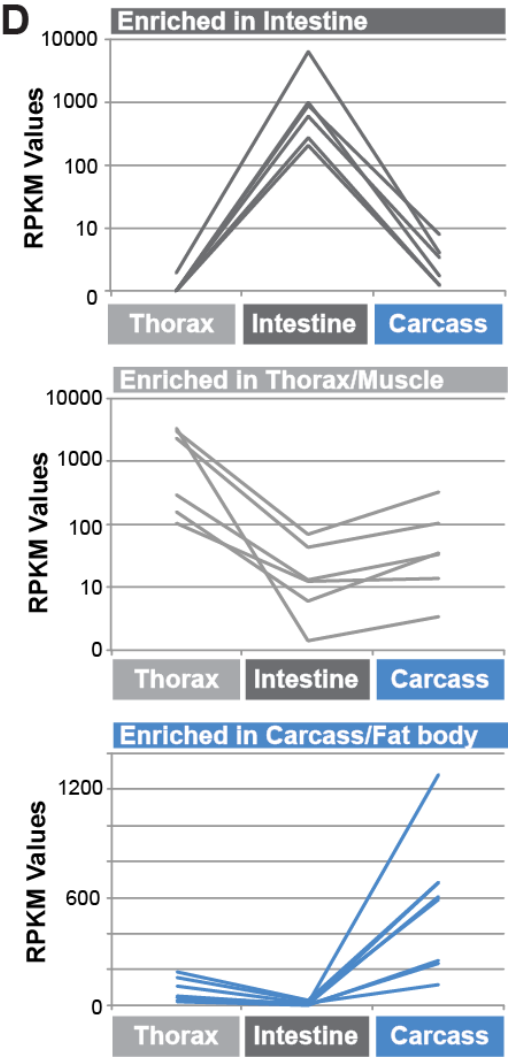

Figure S5

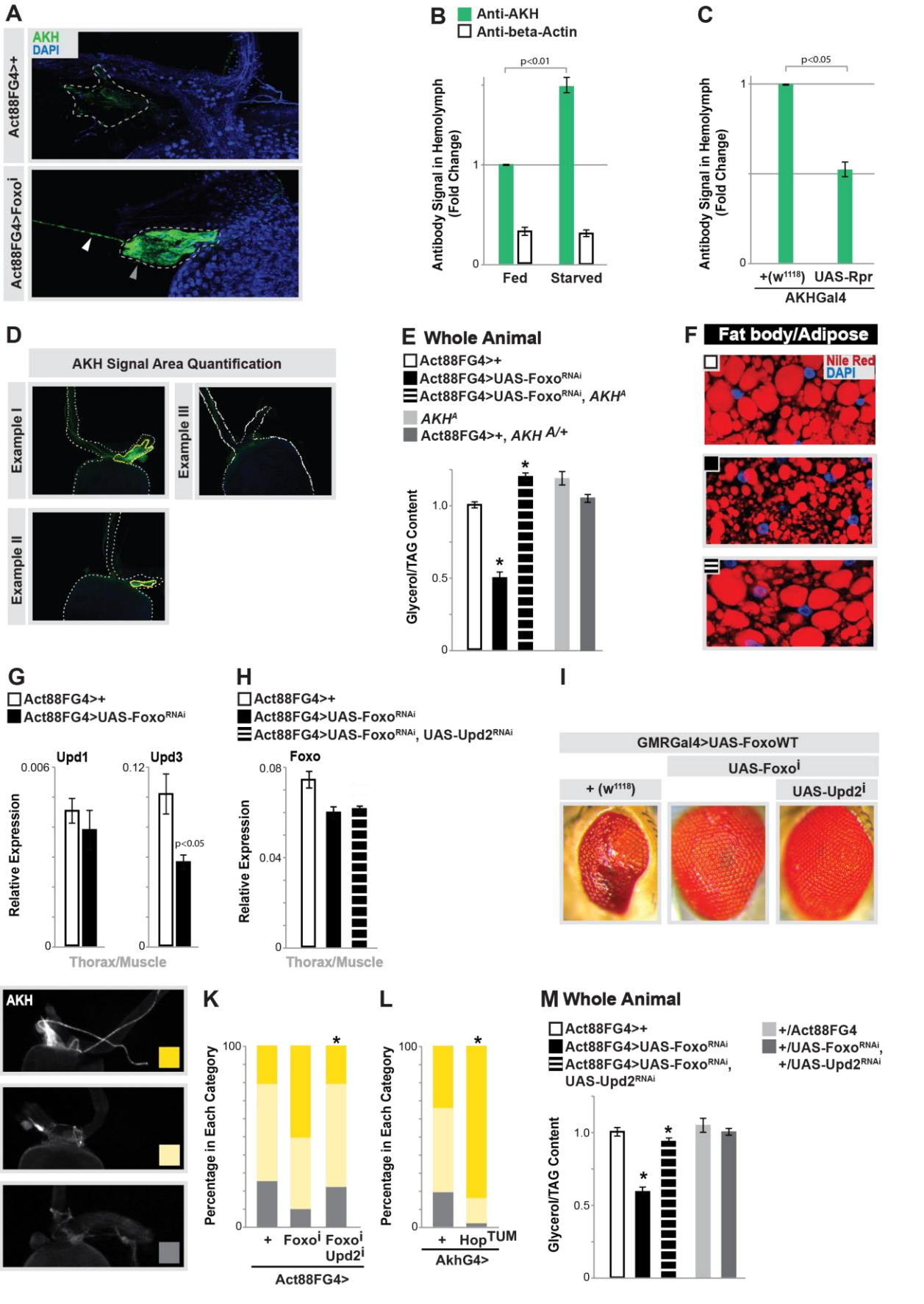
A
AKH
DAPI
Act88FG4>+
Act88FG4>Foxo^i
B
Anti-AKH
Anti-beta-Actin
p<0.01
Antibody Signal in Hemolymph (Fold Change)
Fed
Starved
C
p<0.05
Antibody Signal in Hemolymph (Fold Change)
+(w^1118)
UAS-Rpr
AKHGal4
D
AKH Signal Area Quantification
Example I
Example II
Example III
E Whole Animal
Act88FG4>+
Act88FG4>UAS-Foxo^RNAi
Act88FG4>UAS-Foxo^RNAi, AKH^A
AKH^A
Act88FG4>+, AKH^A/+
Glycerol/TAG Content
F Fat body/Adipose
Nile Red
DAPI
G
Act88FG4>+
Act88FG4>UAS-Foxo^RNAi
Upd1
Upd3
p<0.05
Relative Expression
Thorax/Muscle
H
Act88FG4>+
Act88FG4>UAS-Foxo^RNAi
Act88FG4>UAS-Foxo^RNAi, UAS-Upd2^RNAi
Foxo
Relative Expression
Thorax/Muscle
I
GMRGal4>UAS-FoxoWT
UAS-Foxo^i
+ (w^1118)
UAS-Upd2^i
J
AKH
K
Percentage in Each Category
+
Foxo^i
Foxo^i Upd2^i
Act88FG4>
L
Percentage in Each Category
+
Hop^TUM
AkhG4>
M Whole Animal
Act88FG4>+
Act88FG4>UAS-Foxo^RNAi
Act88FG4>UAS-Foxo^RNAi, UAS-Upd2^RNAi
+/Act88FG4
+/UAS-Foxo^RNAi, +/UAS-Upd2^RNAi
Glycerol/TAG Content

Figure S6

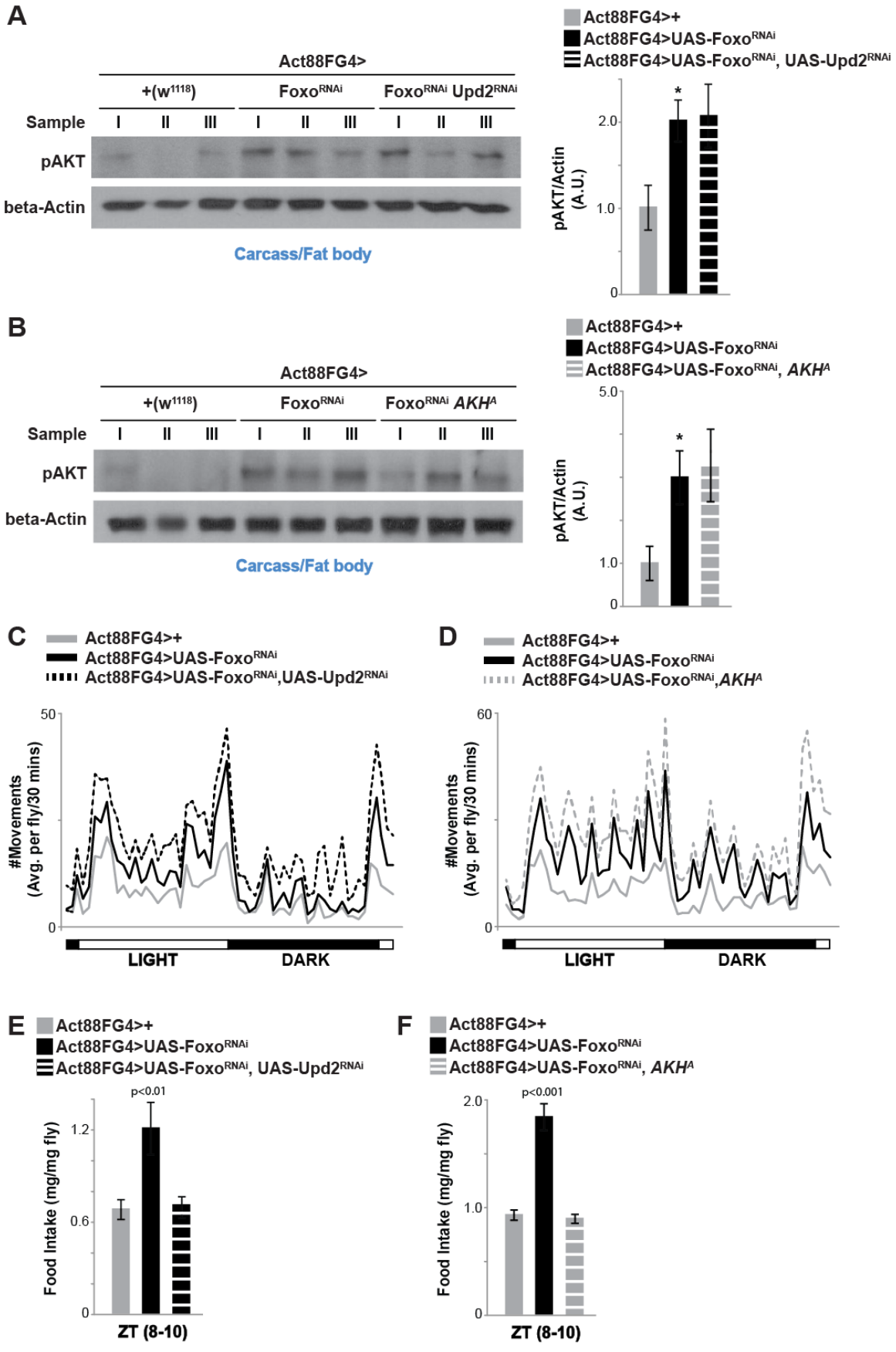
A
Act88FG4>
+(w1118)
FoxoRNAi
FoxoRNAi Upd2RNAi
Sample
I II III I II III I II III
pAKT
beta-Actin
Carcass/Fat body
Act88FG4>+
Act88FG4>UAS-FoxoRNAi
Act88FG4>UAS-FoxoRNAi, UAS-Upd2RNAi
pAKT/Actin (A.U.)
2.0
1.0
0
*
B
Act88FG4>
+(w1118)
FoxoRNAi
FoxoRNAi AKHA
Sample
I II III I II III I II III
pAKT
beta-Actin
Carcass/Fat body
Act88FG4>+
Act88FG4>UAS-FoxoRNAi
Act88FG4>UAS-FoxoRNAi, AKHA
pAKT/Actin (A.U.)
5.0
1.0
0
*
C
Act88FG4>+
Act88FG4>UAS-FoxoRNAi
Act88FG4>UAS-FoxoRNAi,UAS-Upd2RNAi
#Movements (Avg. per fly/30 mins)
50
0
LIGHT
DARK
D
Act88FG4>+
Act88FG4>UAS-FoxoRNAi
Act88FG4>UAS-FoxoRNAi,AKHA
#Movements (Avg. per fly/30 mins)
60
0
LIGHT
DARK
E
Act88FG4>+
Act88FG4>UAS-FoxoRNAi
Act88FG4>UAS-FoxoRNAi, UAS-Upd2RNAi
p<0.01
Food Intake (mg/mg fly)
1.2
0.6
0
ZT (8-10)
F
Act88FG4>+
Act88FG4>UAS-FoxoRNAi
Act88FG4>UAS-FoxoRNAi, AKHA
p<0.001
Food Intake (mg/mg fly)
2.0
1.0
0
ZT (8-10)

Figure S7

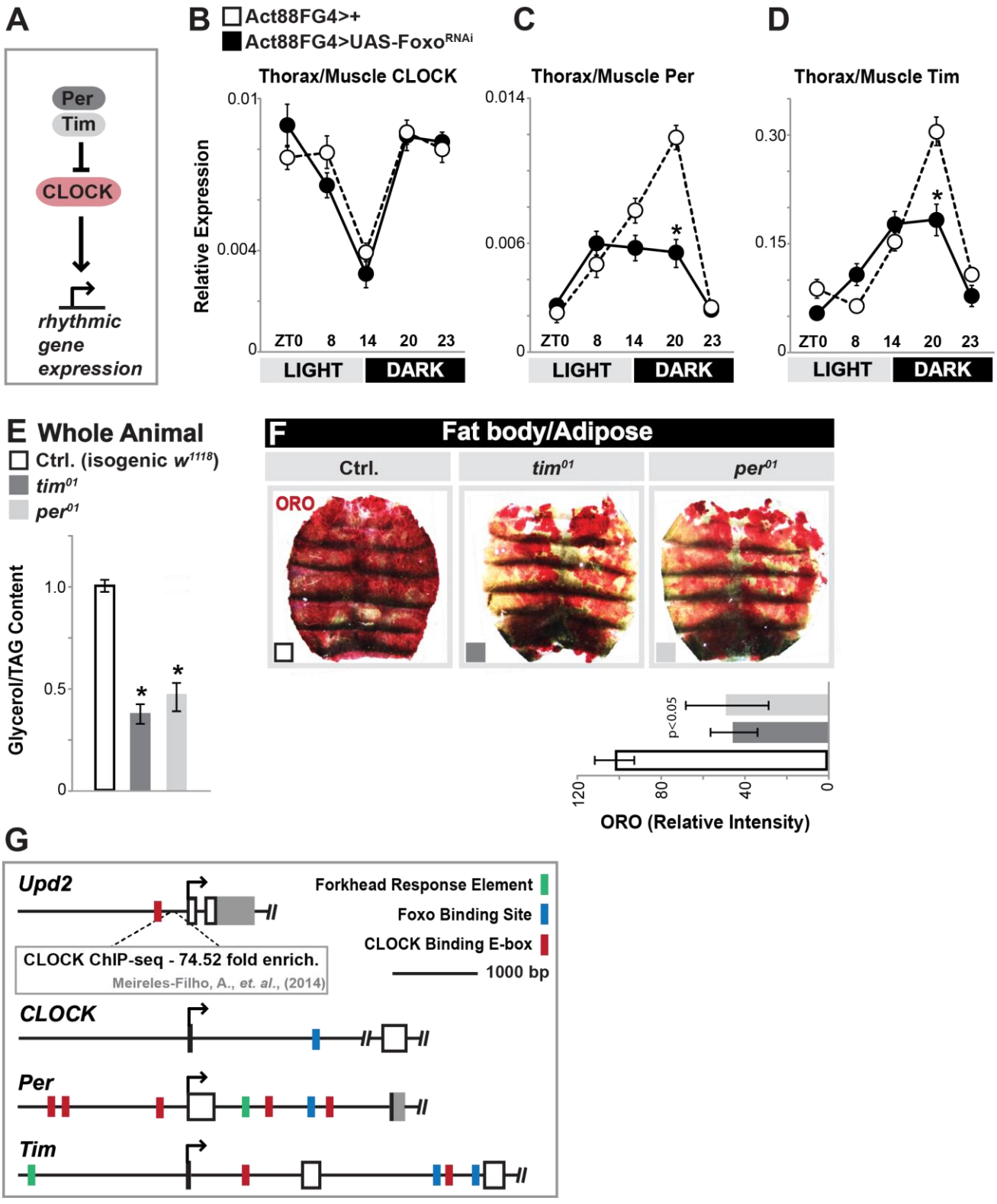
A
Per
Tim
CLOCK
rhythmic gene expression
B
Act88FG4>+
Act88FG4>UAS-Foxo^RNAi
Thorax/Muscle CLOCK
Relative Expression
0.01
0.004
0
ZT0 8 14 20 23
LIGHT DARK
C
Thorax/Muscle Per
0.014
0.006
0
ZT0 8 14 20 23
LIGHT DARK
D
Thorax/Muscle Tim
0.30
0.15
0
ZT0 8 14 20 23
LIGHT DARK
E Whole Animal
Ctrl. (isogenic w1118)
tim01
per01
Glycerol/TAG Content
1.0
0.5
0
F Fat body/Adipose
Ctrl.
tim01
per01
ORO
p<0.05
120
80
40
0
ORO (Relative Intensity)
G
Upd2
CLOCK ChIP-seq - 74.52 fold enrich.
Meireles-Filho, A., et. al., (2014)
Forkhead Response Element
Foxo Binding Site
CLOCK Binding E-box
1000 bp
CLOCK
Per
Tim

Figure S1: Muscle-dependent changes in organismal lipid homeostasis. Related to Figure 1.

(A) Lipid transport from fat body is required for neutral lipid storage in the thorax/muscle. Attenuating Drosophila lipoproteins Lpp; lipophorin and LTP; Lipid Transfer Particle; utilizing RNAi) in adult fat body (using the temperature sensitive driver PplGal4, tubG80^{ts}; TARGET system) significantly decreases TAG levels in dissected thorax/muscle, but not the abdomen. n=5 samples.

(B) Act88FGal4 driver specificity [S1]. Act88FGal4 is active (utilizing UAS-nlsGFP) almost exclusively in the thoracic muscle, including the longitudinal indirect flight muscles (IFM), dorsal lateral muscles, dorsal ventral muscles, and weaker expression in leg muscles. GFP expression is also observed, although much weaker, in the muscle underlying the proboscis. No GFP expression is observed in any tissue in the carcass. Driver becomes active after development of thoracic muscle in late pupal stages.

(C) Act88FGal4 is not active in the visceral muscle of the midgut (muscle nuclei marked by vein-lacZ (vn-LacZ, white); actin filaments/muscle (Phalloidin (Phall, red); and nuclei (DAPI, blue).

(D-F) Muscle-specific Foxo depletion in males leads to lipid metabolic deficits

(D) Starvation sensitivity of males upon Foxo depletion (RNAi line v106097) in muscle using Act88FGal4

(E) Total triglycerides (TAG) levels of whole males; n=5 samples.

(F) Oil red O (ORO) neutral lipid stain of male fat body.

(G-H) Immunostaining to detect lipid droplets (LD) in dissected longitudinal thoracic muscle (IFM) using a lipid droplet binding domain-GFP fusion protein (UAS-LD-GFP). The majority of LD-GFP marked LDs (green, forms ring around droplet) overlap with neutral lipid stain nile red (red, see gray arrow as example). LD-GFP also marks muscle nuclei (DAPI, blue), which are negative for nile red stain (white arrow). LD-GFP marked LDs also associate with mitochondria (H, mitochondria marked by MitoTracker (red)).

(I) LD-GFP marked LDs respond to increases in catabolic activity. Over-expressing Drosophila Bmm (homolog of ATGL, triglyceride lipase) in muscle results in drastic decreases in LD-GFP lipid droplets.

(J-M) Foxo depletion using MHCGal4 phenocopies Act88FGal4

(J) Total triglycerides (TAG) levels of whole females upon Foxo depletion (RNAi line v106097) in muscle using MHCGal4; a ubiquitous, muscle specific driver. n=6 samples.

(K) Starvation sensitivity of female flies.

(L) Oil red O (ORO) neutral lipid stain of intestines.

(M) Nile red stain (for LD) of fat body; nile red (red) and DAPI (blue) detected by immunostaining.

All bars represent mean±SE. Controls animals represent PplGal4,tubG80^{ts}>UAS-Luciferase^{RNAi}, Act88FGal4>+(w^{1118}), and MHCGal4>+(w^{1118}).

Figure S2: Muscle-specific Foxo function is required to maintain systemic lipid homeostasis. Related to Figures 1 and 2.

(A) Foxo RNAi efficiency. Over-expressing wild-type Foxo in the developing eye (GMRGal4>UAS-FoxoWT) results in an apoptotic phenotype (left panels). Inhibiting Foxo with RNAi transgene VDRC 106097 in the genetic background can completely rescues the apoptotic phenotype, while inhibiting Foxo with RNAi transgene TRiP HMS00793 (i(T)) partially rescues the apoptotic phenotype.

(B-D) Changes in lipid homeostasis upon muscle-specific depletion of Foxo (RNAi HMS00793)

(B) Total triglycerides (TAG) levels of whole females upon Foxo depletion (i(T)) in muscle using Act88FGal4. n=6 samples.

(C) Oil red O (ORO) neutral lipid stain of intestines. Intensity quantification of ORO, n=15 samples.

(D) ORO stain and nile red stain (for LD) of fat body; nile red (red) and DAPI (blue) detected by immunostaining. Intensity quantification of ORO, n=6 samples.

(E-G) UAS-FoxoRNAi transgene (v106097) alone does not affect lipid homeostasis. Total TAG levels of whole females (n=5 samples), as well intestinal ORO stain (and quantification, n=12 samples), from UAS-FoxoRNAi/+(w^{1118}) and +/+(w^{1118}) female siblings.

All bars represent mean±SE. All experiments represent female flies. Controls animals for experiments with Act88FGal4>UAS-Foxoi(T) represent genetically matched Act88FGal4>UAS-LuciferaseRNAi.

Figure S3: Behavioral, developmental, and insulin activity changes associated with muscle-specific depletion of Foxo. Related to Figures 1-4, 7.

(A) Analysis of muscle structure upon Foxo depletion (RNAi line v106097) in muscle using Act88FGal4. Immunostaining of myofibrils from dissected longitudinal thoracic muscle (IFM). Phalloidin, (Phall, green) stains actin fillaments and actinin (red) stains Z-lines.

(B) Foxo depletion in muscle results in increased climbing ability. n=5 cohorts of 20 flies.

(C-D) Foxo depletion in muscle results in increased food intake. Act88FGal4>UAS-FoxoRNAi flies display increase food intake using both the Blue Dye feeding assay (C, n=6 cohorts of 5 flies) and the CAFE assay (D, n=8-10 samples). Note: Act88FGal4>UAS-FoxoRNAi flies only display a significant increase in intake (using the Blue Dye assay) in the light cycle (ZT(8-10), 8-10 hours after lights ON).

(E) Measurement of rhythmic activity upon muscle-specific depletion of Foxo. Each 30 min. time-point averaged represents 8-12 individual flies. Note: Act88FGal4>UAS-FoxoRNAi flies display similar rhythms compared to control flies, especially in regard to shifts in activity during light/dark cycle transitions. Act88FGal4>UAS-FoxoRNAi flies also display a trend (although not significant) of enhanced movements.

(F) No change in weight (n=13-16 samples) or size (length, representative images selected) of adult flies upon muscle-specific depletion of Foxo.

(G-H) Changes in lipid storage (Oil red O (ORO) neutral lipid stains) of intestines and fat bodies at Day 2, 5, and 10 post-eclosion (adulthood) upon muscle-specific depletion of Foxo. Intensity quantification of ORO, n=8-10 samples.

(I) Drosophila insulin-like peptides *dilp2*, *dilp3*, and *dilp5* transcription (measured by qRT-PCR) in dissected heads upon muscle-specific depletion of Foxo. n=4 samples

(J) pAKT (phosphor AKT) levels in dissected carcass/fat body upon muscle-specific depletion of Foxo; independent samples labeled I, II, and III. Quantification of three independent samples; A.U. – arbitrary units. Samples were taken at ZT(8-10).

All bars represent mean±SE. All experiments represent female flies. All control animals represent Act88FGal4>+(w^{1118}).

Figure S4: Unique tissue transcriptomes. Related to Figure 2.

(A-B) RPKM values for select, basally high genes that show no change upon muscle-specific depletion of Foxo in all of the unique tissue transcriptomes (thorax/muscle; intestine; carcass/fat body). Plotted on graph (B); log scale; each line represents a unique gene.

(C-D) Tissue-specific gene expression of transcriptomes generated from dissected thorax/muscle, intestine, and carcass/fat body of control (Act88FGal4>+(w^{1118}). RPKM values for select genes (in which tissue-specificity has been previously characterized or identified) enriched in various dissected samples. RPKM values for all genes listed are given for all tissue-types; high RPKM values highlighted in red, and low RPKM values highlighted in green (red/green heat maps represent select groups of genes designated by dotted gray line). Genes enriched in the intestine (top group), thorax/muscle (middle group), and carcass/fat body (bottom group) are plotted on graphs (D); each line represents a unique gene. These data highlight the tissue-specificity of the various transcriptomes.

Figure S5: AKH and Upd2 are required for muscle-dependent changes in systemic lipid homeostasis. Related to Figures 4-6.

(A) Enhanced images displaying AKH immunostaining of corpora cardiaca (CC) cell bodies (gray arrow) and associated axons (white arrow); AKH (green) and DAPI (blue). General CC structure is outlined (dotted gray line). Anti-AKH signal is generally weak or absent in control flies (Act88FGal4>+(w^{1118}), and widespread in Act88FGal4>UAS-FoxoRNAi (RNAi line v106097) flies. Note: AKH immunostaining of axons did not always correlate with increased AKH immunostianing within CC cells.

(B) Quantification of anti-AKH signal in isolated hemolymph after acute starvation (16 hours) in control flies (Act88FGal4>+(w^{1118})) using EIA; fold change. Anti-beta-Actin was used as a negative control to confirm the absence of hemocytes (cells) in isolated hemolymph; fold change compared to Fed anti-AKH signal. n=4 samples.

(C) Quantification of anti-AKH signal in isolated hemolymph after ablation of AKH-producing cells (AKHGal4>UAS-Reaper(Rpr)) compared to control flies (AKHGal4>+(w^{1118})) using EIA; fold change. n=4 samples.

(D) Examples of sample images used to quantitate AKH signal area in CC using ImageJ. Anterior proventriculus and crop duct highlighted by dotted white line; CC and AKH signal (green) highlighted by yellow dotted line.

(E) Total triglycerides (TAG) levels of whole flies upon Foxo depletion in muscle (Act88Gal4) in various genetic backgrounds related to changes in AKH signaling. Values for Act88FGal4>+(w^{1118}), Act88FGal4>UAS-FoxoRNAi, and Act88FGal4>UAS-FoxoRNAi; AKH^{A} are identical to those presented in Fig. 4D. AKH^{A} (independent mutant) and Act88FGal4>+(w^{1118}), AKH^{A} /+ represent additional controls. Note; AKH^{A} mutants have elevated TAG levels compared to various controls, and Act88FGal4>UAS-FoxoRNAi; AKH^{A} rescue TAG levels to similar levels. n=5 samples.

(F) Nile red stain (for LD) of fat body (nile red (red) and DAPI (blue) detected by immunostaining) in Act88FGal4>+(w^{1118}) controls, Act88FGal4>UAS-FoxoRNAi, and Act88FGal4>UAS-FoxoRNAi; AKH^{A} rescue flies.

(G) *upd1* and *upd3* transcription (measured by qRT-PCR) in dissected thorax/muscle upon muscle-specific depletion of Foxo, n=6 samples.

(H) *foxo* transcription (measured by qRT-PCR) in dissected thorax/muscle upon muscle-specific depletion of Foxo (Act88FGal4>UAS-FoxoRNAi) and concurrent depletion of Upd2 (Act88FGal4>UAS-FoxoRNAi, UAS-Upd2RNAi), n=6 samples.

(I) Foxo RNAi efficiency within the Upd2RNAi genetic background. Over-expressing wild-type Foxo in the developing eye (GMRGal4>UAS-FoxoWT) results in an apoptotic phenotype (left panels). Inhibiting Foxo with RNAi in the genetic background can completely rescue the apoptotic phenotype, even while concurrently inhibiting Upd2 with RNAi (UAS-Upd2RNAi).

(J-L) Quantification of corpora cardiaca (CC) AKH immunostain upon; (K) muscle-specific depletion of Foxo (Act88FGal4>UAS-FoxoRNAi) and rescue with concurrent depletion of Upd2 (Act88FGal4>UAS-FoxoRNAi, UAS-Upd2RNAi); and (L) upon over-activation of Hop (HopTumL) in CC AKH-producing cells (AKHGal4>UAS-HopTumL). n=10-15 samples; *p-value<0.01.

(M) Total triglycerides (TAG) levels of whole flies upon Foxo depletion muscle (Act88Gal4) in various genetic backgrounds related to changes in Upd2 activity. Values for Act88FGal4>+(w^{1118}), Act88FGal4>UAS-FoxoRNAi, and Act88FGal4>UAS-FoxoRNAi; UAS-Upd2RNAi are identical to those presented in Fig. 6A. +(w^{1118})/Act88FGal4 and +(w^{1118})/UAS-FoxoRNAi; +(w^{1118})/Upd2RNAi represent additional controls. n=5 samples.

All bars represent mean±SE. All experiments represent female flies except for panel I.

Figure S6: Uncoupling hyperactivity, elevated insulin function, and hyperphagia from the Foxo/Upd2/AKH communication axis. Related to Figures 6-7.

(A) pAKT (phospho AKT) levels in dissected carcass/fat body upon muscle-specific depletion of Foxo (Act88FGal4>UAS-FoxoRNAi) and with concurrent depletion of Upd2 (Act88FGal4>UAS-FoxoRNAi, UAS-Upd2RNAi); independent samples labeled I, II, and III. Attenuation of Upd2 does not rescue Foxo-mediated changes in insulin activity. NOTE: Control (Act88FGal4>+(w^{1118})) and Act88FGal4>UAS-FoxoRNAi samples are identical to those represented in Fig. S3. Right panel; Quantification of three independent samples, A.U.–arbitrary units. Samples were taken at ZT(8-10).

(B) pAKT (phospho AKT) levels in dissected carcass/fat body upon muscle-specific depletion of Foxo (Act88FGal4>UAS-FoxoRNAi) and with concurrent depletion of AKH (Act88FGal4>UAS-FoxoRNAi, AKH^{A}); 3 of 5 independent samples shown, labeled I, II, and III. Attenuation of AKH does not rescue Foxo-mediated changes in insulin activity. Right panel; Quantification of five independent samples, A.U.–arbitrary units. Samples were taken at ZT(8-10).

(C) Measurement of rhythmic activity upon muscle-specific depletion of Foxo (Act88FGal4>UAS-FoxoRNAi) and with concurrent depletion of Upd2 (Act88FGal4>UAS-FoxoRNAi, UAS-Upd2RNAi). Each 30 min. time-point averaged represents 10-11 individual flies. Note: Both genotypes display similar rhythms compared to control flies, especially in regard to shifts in activity during light/dark cycle transitions. However, attenuation of Upd2 does not rescue Foxo-mediated changes in hyperactivity.

(D) Measurement of rhythmic activity upon muscle-specific depletion of Foxo (Act88FGal4>UAS-FoxoRNAi) and with concurrent depletion of AKH (Act88FGal4>UAS-FoxoRNAi, AKH^{A}). Each 30 min. time-point averaged represents 10-11 individual flies. Attenuation of AKH does not rescue Foxo-mediated changes in hyperactivity.

(E-F) Act88FGal4>UAS-FoxoRNAi flies display increased food intake (using the Blue Dye feeding assay (n=5-6 cohorts of 5 flies)) that can be rescued with concurrent depletion of (E) Upd2 (Act88FGal4>UAS-FoxoRNAi, UAS-Upd2RNAi) or (F) AKH (Act88FGal4>UAS-FoxoRNAi, AKH^{A}). Samples were taken in the light cycle at (ZT(8-10), 8-10 hours after lights ON). All bars represent mean±SE. All experiments represent female flies. All control animals represent Act88FGal4>+(w^{1118}).

Figure S7: Circadian control of the Foxo/Upd2/AKH communication axis. Related to Figure 7.

(A) CLOCK (transcription factor) is an essential activator of circadian rhythmic gene expression. Per (period) and Tim (timeless) heterodimers (whose expression is regulated by CLOCK) inhibit CLOCK transcription factor DNA binding.

(B-D) Diurnal abundance of *CLOCK, per, and tim* transcription (measured by qRT-PCR) in dissected thorax/muscle from in Act88FGal4>+(w^{1118}) control and Act88FGal4>FoxoRNAi flies. Note: CLOCK mRNA is regulated anti-phasic to Per and Tim mRNA. Muscle-specific Foxo depletion does not affect

diurnal abundance of *CLOCK*, but is required for rhythmic expression of *per* and *tim.* n=5 samples. *p-value<0.01, designates ZT data point for Act88FGal4>FoxoRNAi is significantly changed compared to corresponding ZT data point for controls.

(E) Attenuation of total triglycerides (TAG) levels in timeless mutant (tim^{01}) and period mutant (per^{01}) flies; whole flies compared to isogenic (w^{1118}) controls, n=5 samples.

(F) Attenuation of lipid storage (Oil red O (ORO) neutral lipid stains) in fat body of timeless mutant (tim^{01}) and period mutant (per^{01}) flies; compared to isogenic (w^{1118}) controls. Intensity quantification of ORO, n=6-8 samples.

(G) Classical Foxo DNA binding motifs (Forkhead Response Elements and Foxo Binding Sites) are not present in the promoter of Upd2, but are present in promoter/enhancer regions of CLOCK, Per, and Tim. CLOCK binding E-box motif is present in the promoter of Upd2; via ChIP-Seq., CLOCK binding is over 70 fold enriched in the Upd2 promoter [S2].

Primer	Sequence (5'-3')
ACC F	CTATCGCTATGGTTACCTGCCGTA
ACC R	AACATGATCTGTGTGCCACCCAAC
FASN1 F	TGATGGCCGGTATTCTGGAAGAGA
FASN1 R	ATTGCTCATCAGCTCAGCGAACCT
Yip2 F	CGGTCTTAAGGGTGAGCAAG
Yip2 R	ACATTACGGGCAATGAAAGG
Bmm F	CAATAAGGGTCTGGCCAACTGGAT
Bmm R	TAAGTCCTCCACCATTACTCTGGC
Mondo F	CGCCTCTGAACGATAGGAAC
Mondo R	CTTCTGGAACTGGAGGCAAG
Thor F	CACTTGCGGAAGGGAGTACG
Thor R	TAGCGAACAGCCAACGGTG
Dilp2 F	TCCACAGTGAAGTTGGCCC
Dilp2 R	AGATAATCGCGTCGACCAGG
Dilp3 F	AATCCTTATGATCGGCGGTG
Dilp3 R	TACGTTCTCGGCTTGGCAG
Dilp5 F	GCTCCGTGATCCCAGTTCTC
Dilp5 R	GAGTCGCAGTATGCCCTCAAC
Upd2 F	CCACAACCTGCGACTCTTCT
Upd2 R	GCGCGGTGGGTTATATCTT
Upd1F	AATCAGCTGAAGCGCCACG
Upd1 R	GGAATTGGGCTTGAGCTTGG
Upd3 F	GCGGGGAGGATGTACC
Upd3 R	GTCTTCATGGAATGAGCC
CLOCK F	CAGTTCAACTCGCTGGTCAA
CLOCK R	ACCATCGAGAGACTCCAGCA
Per F	AACGGTTGCTACGTCCTTCT
Per R	CGCTTCACGATATCCTCCTT
Tim F	AGTCGCCACTCACCATTCCT
Tim R	TTCAGCTTGTTGCCGTTGT

Table S1: Primer sequences used for qRT-PCR. Relates to Figures 2, 3, 5, 7, S3, S5, and S7.

Supplemental References

S1. Nongthomba, U., Pasalodos-Sanchez, S., Clark, S., Clayton, J.D., and Sparrow, J.C. (2001). Expression and function of the Drosophila ACT88F actin isoform is not restricted to the indirect flight muscles. J Muscle Res Cell Motil 22, 111-119.

S2. Meireles-Filho, A.C., Bardet, A.F., Yanez-Cuna, J.O., Stampfel, G., and Stark, A. (2014). cis-regulatory requirements for tissue-specific programs of the circadian clock. Curr Biol 24, 1-10.